ISSN: 2688-8645

# Safety Analysis of Offshore Wells Plugging and Abandonment Process with Riserless Well Intervention System Using a DBN based Comprehensive Method

Chuan Wang[1, 2, *], Jianjun Luo[1, 2], Huachuan Liu[1, 2], Xueliang Zhang[1, 2]

[1]School of Mechatronic Engineering, Southwest Petroleum University, Chengdu, Sichuan, 610500, China

[2]Energy Equipment Research Institute, Southwest Petroleum University, Chengdu, Sichuan, 610500, China

*Corresponding author

## Abstract

**The Riserless Well Intervention (RLWI) system that performs complex offshore oil well Plugging and Abandonment (P&A) operations is a typical Multi-Mission Phased-Mission System (MM-PMS), which requires multiple missions to be completed within a phase. P&A processes involve complex operations and equipment that can contaminate local marine ecosystems if they fail. Therefore, it is necessary to evaluate the reliability of the RLWI system. This paper proposes a dynamic reliability evaluation model for analyzing the RLWI MM-PMS. The GO model of the phase operation process and the Fault Tree (FT) model used to analyze the failure of each mission were established, and a Dynamic Bayesian Network (DBN) model based on the GO model and the FT model was developed for reliability evaluation. The established model can analyze the changes in the reliability of the RLWI MM-PMS more comprehensively, and can also clarify the importance of different missions and different system components. In addition, considering the impact of the marine environment on operators, the Standardized Plant Analysis Risk-Human (SPAR-H) reliability analysis is used for quantification. These findings can guide the improvement of the reliability of the RLWI system and the success rate of P&A operations.**

## Keywords

**Safety Analysis; Reliability; Riserless Well Intervention System; Plugging and Abandonment; Dynamic Bayesian Network; Standardized Plant Analysis Risk-Human.**

## 1. Introduction

When an oil well has uncontrollable leakage, structural failure, or production is not profitable, it will be permanently Plugging and Abandonment (P&A) (Standard, 2004). The Riserless Well Intervention (RLWI) system is used to perform comprehensive P&A operations for simple and moderately complex oil wells (Øia et al., 2018). If the P&A operation fails, the leaked oil will cause serious pollution to the local marine ecological environment. The P&A operation of the Elgin oil well in 2013 and the G-4 oil well of Troll Field in 2016 failed. The leaked crude oil not only polluted a large area of the nearby sea but also spent a lot of money on environmental management and relaunch of rescue P&A work (Babaleye et al., 2019). The current research on P&A operations is mainly aimed at estimating the operation time and cost (Moeinikia et al., 2015), and determining the cause and probability of leakage after the operation is completed (Babaleye et al., 2019). Therefore, it is necessary to evaluate the reliability of the RLWI MM-PMS to improve the success rate of P&A operations.

ISSN: 2688-8645

The P&A operation consists of four different phases: the preparatory phase, reservoir abandonment phase, intermediate abandonment phase, and wellhead and conductor removal phase (Øia et al., 2018). The first three phases include multi-mission. The RLWI system that performs P&A operations is a typical Multi-Mission Phased-Mission System (MM-PMS). The biggest difference from traditional Phased-Mission Systems (PMSs) such as aerospace systems and sensor network communication systems is that multiple missions need to be completed in a specific phase (Peng et al., 2019). Therefore, RLWI System not only has the characteristics of different configurations of PMS in different phases and the phase dependence of components but also has the characteristics of multi-mission in phases. These characteristics make the reliability analysis of the RLWI system more difficult.

So far, many methods have been proposed to analyze the reliability of PMS. These methods can be divided into two main categories. The first category is the state-space-based approach, such as Markov chains and their extension methods (Alam and Al-Saggaf, 1986) and Petri nets (PNs) (Mura and Bondavalli, 2001). Although these methods can model and analyze complex systems, they suffer from the state-space explosion and cannot be used in large-scale RLWI MM-PMS systems. The second category is the combinatorial method, including various decision diagram methods derived from decision diagram theory (Tang and Dugan, 2006) and the Fault Tree Analysis (FTA) (La Band and Andrews, 2004) method. These methods can effectively analyze large-scale systems, but cannot effectively analyze the dynamic changes of the RLWI MM-PMS.

Yet, the classical probabilistic graphical model Bayesian network (BN) and its time-expanded dynamic Bayesian network (DBN) can clearly express the logical relationships within a single phase and the dependencies of different phases (Xu et al., 2019). It can also predict the change of system reliability over time (Liu et al., 2020). For example, Liu et al. (Liu et al., 2008) used BN to analyze the reliability of PMS. Xu et al. (Xu et al., 2019) used DBN and Expectation-Maximization to successfully evaluate the reliability of multi-state phased-mission systems by fusing data from multiple phases with each other. In addition, DBN is also widely used in complex marine engineering and process systems. Liu et al. (Liu et al., 2021) comprehensively considered the risk factors leading to blowout accidents. A dynamic risk assessment model based on DBN was developed to assess the safety of deepwater drilling operations. Wang et al. (Y. Wang et al., 2021) established a DBN prediction model for the reliability of emergency evacuation on offshore platforms. The changes in the reliability of the evacuation process are analyzed and the main reasons leading to the failure of emergency evacuation are determined. Li et al. (Li et al., 2021) considered the dynamic characteristics and uncertainty of pipeline fatigue failure and developed a dynamic method based on DBN to evaluate the fatigue failure probability of spanning pipelines in real time. Khakzad et al. (Khakzad et al., 2013) mapped the bow-tie to BN, and used probability adaptation to dynamically correct the prior probability of the accident component. The limitation of the bow-tie analysis in the dynamic safety analysis of the processing system is solved.

For RLWI MM-PMS that needs to complete multiple missions in certain specific phases. This article uses the GO method to analyze and model the phase with multi-mission. The GO method is a success-oriented method. The basic idea is to translate a system schematic or flowchart directly into a GO diagram according to certain rules for reliability analysis of complex systems with time series (Matsuoka and Kobayashi, 1988). Nie et al. (Nie et al., 2019) used the GO method to convert the operation flowchart of riser emergency disconnect at different stages into the corresponding GO model and then combined it with DBN to predict the dynamic success probability of different stages. Wang et al. (C. Wang et al., 2021) developed a GO model to prevent secondary generation during offshore gas hydrate production, predicted the performance of the gas hydrate production system, and analyzed the risks in the production process by DBN. Liu et al. (Liu et al., 2018) developed a GO model for the shutdown of the

ISSN: 2688-8645

blowout preventer process and analyzed the risk of subsea blowout preventer with BN. In summary, the GO approach is well suited for modeling multi-mission phase processes.

RLWI system involves a large number of components in the process of P&A operations. To determine the root component failure that caused the system failure and mission failure, quickly locate the fault location to simplify subsequent maintenance activities. FTA, the widely used system failure analysis method (Bobbio et al., 2001), is used to model potential risks in the process of system execution. Another issue that needs attention is that the participation of personnel is inevitably required when using the system to complete various missions. Therefore, human reliability has a non-negligible impact on the reliability of a system or mission. The existing Human Reliability Analysis (HRA) is categorized into three generations. The first generation of HRA methods focus on the external behavior of human and ignored the cognitive mechanism of the internal behavior, which makes the prediction results more subjective and lacks accuracy. Such as the Success Likelihood Index Method (Hameed et al., 2016) and the Technique for Human Error Rate Prediction (Purba and Tjahyani, 2016). The second generation methods such as Cognitive Reliability and Error Analysis Method (CREAM) (Desmorat et al., 2013), A Technique for Human Error Analysis (ATHEANA) (Cooper et al., 1996), and Standardized Plant Analysis Risk-Human (SPAR-H) Reliability Analysis Method. The disadvantage of ATHEANA is that it requires a large team, and different teams may produce the same results (Forester et al., 1998). Although CREAM can transform expert judgment data into quantitative human failure analysis, it cannot accurately obtain the probability of human error (Wang et al., 2011). Then, the Standardized Plant Analysis Risk-Human (SPAR-H) Reliability Analysis is one of the representative second-generation HRA methods. The method pays more attention to the influence of environmental and situational factors on the probability of human error, which has been widely applied in the industry (Jahangiri et al., 2016). SPAR-H divides human activities into diagnosis and operation. Different levels of eight performance shaping factors (PSF) and calculation equations for different activities are defined to estimate human error probabilities (HEPs). This makes the assessment process much easier for those involved (Vaez and Nourai, 2013). The third-generation HRA method is based on the research of the previous two generations of HRA methods and is combined with cognitive psychology, neuroscience, and other multidisciplinary knowledge. However, no public data is currently available (Chen et al., 2019).

To fill the research gaps, this paper proposes an integrated DBN-based approach to analyze the reliability of RLWI MM-PMS. The potential contributions of this method are as follows: (1) The P&A operation process that contains multiple missions is continuous, and the interaction between multiple missions is defined. (2) Hierarchical division of RLWI components used in different missions is convenient for inspection and maintenance, (3) Obtain the dynamic changes of the reliability of RLWI system in the P&A process. The GO method is applied to convert the single-phase multi-mission flowchart into the corresponding GO model. The FTA is used to obtain the corresponding fault tree (FT) model. During the execution of each mission, the components' failure that causes the mission's fail is determined. Then, the GO model of each phase and the FT model of each mission in that phase are merged according to the rule mapping. The BN-GO-FT model for each phase is obtained. The SPAR-H method is used to calculate the probability of operator failure, taking into account the human factor. The accuracy of the model can be further improved by adding human factors to the model. The output of the previous phase is used as the input for the next phase. Combining the runtime requirements of each phase, the final all-phase DBN-GO-FT model of MM-PMS is obtained. After determining the state probability values of all nodes, the DBN can be used to analyze the reliability of the RLWI MM-PMS over time.

The rest of the paper is structured as follows. Section 2 briefly introduces the characteristics of MM-PMS. Section 3 presents the reliability assessment method of MM-PMS based on DBN and

ISSN: 2688-8645

describes the modeling process in detail. Section 4 builds a dynamic BN model for evaluating the reliability of RLWI MM-PMS. Section 5 presents an analysis of the results. Conclusions are given in Section 6.

## 2. MM-PMS Descriptions

MM-PMS is composed of multiple consecutive and non-overlapping phases. The work time of each phase is determined separately. At some phases, multiple missions may need to be completed. The equipment composition of MM-PMS has a certain level. As the mission type changes and time advances, the subsystems and components of the system dynamically join, continue, and exit. Therefore, each mission has a corresponding component configuration. The state of these components is generally considered to be phase-dependent. Only when multiple missions in the phase and all phases are successfully executed in order, the entire MM-PMS task is considered to be successfully executed. The rest will be regarded as an overall task failure. A concise example of MM-PMS is shown in Fig. 1. The system contains three components: U1, U2, and U3. The black directed arrow indicates that the component is used in this mission, while the gray one indicates that the component is not used in this mission.

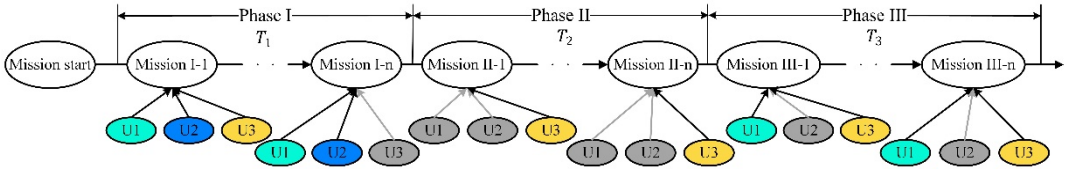


**Fig 1.** MM-PMS concise example diagram.

To facilitate the evaluation of the reliability of MM-PMS. The assumptions of this paper are as follows (Xu et al., 2019).

(1) There are only two states for system components: normal and fault, which are not repaired during the work.

(2) The failure modes of each component or subsystem of the system are independent of each other. The hydraulic and electronic components in the RLWI system, such as valves, usually follow an exponential distribution. The lifespan of some mechanical components obeys the Weibull distribution. Offshore and Onshore Reliability Data (OREDA) counts the failure rates of these components and obtains a constant failure rate. This means that the life of mechanical components also obeys an exponential distribution.

(3) At the beginning of the mission, the normal state probability of the system components is 1 and the fault state probability is 0.

(4) The phase dependency of a system component is defined as the state when the end of the previous phase is used as the initial state of the next phase of the same component. All components in the system are independent of each other. Due to the phase dependence, the initial state of each component at the next phase is the same as the state of the component at the end of the previous phase.

## 3. Reliability Modeling and Analysis Methods

This section proposes a comprehensive method based on DBN to analyze the reliability of MM-PMS. The structural framework of the proposed integrated method is shown in Fig. 2, which consists of five main modules as described below.

ISSN: 2688-8645


**Fig 2.** The structural framework of the MM-PMS reliability analysis method.

## 3.1. Module 1: Analysis MM-PMS

Before analyzing the reliability of MM-PMS, it is necessary to clarify the missions included in each phase and the corresponding mission flow. In addition, it is useful to analyze the components or subsystems of the system to facilitate FT modeling.

## 3.2. Module 2: GO Model for Each Phase

In this paper, the GO approach is used to model phases in MM-PMS that contain multiple missions. The two major elements of GO graphs are operators and signal flow (Zupei et al., 2001). Operators represent events, and the direction of signal flow reflects the sequence and correlation between events. The number in the operator in the GO graph can be represented by M-i, where M means the type of the operator, and i means the number of the operator. In Fig. 3, S means input signal and R means output signal. The GO method has defined 17 standard operators (Liu et al., 2015). The choice of operator type is based on the mission type. Take the concise example diagram of MM-PMS in Fig. 1 as an example, the type 5 operator indicates the start of the task, while the type 1 operator indicates the mission in the phase. Using the signal flow to connect the operators in turn, the final GO model of the concise example of MM-PMS is shown in Fig. 3. It should be noted that the last operator 1-(3n+1) in Fig. 3 indicates the end of the task.

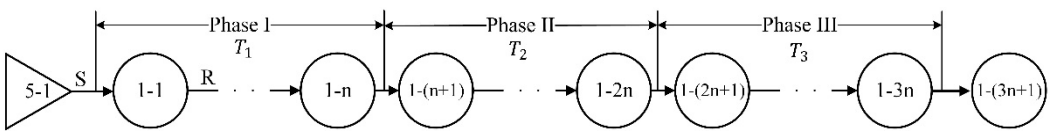


**Fig 3.** The GO model of MM-PMS concise example diagram.

ISSN: 2688-8645

## 3.3. Module 3: FT Model for Each Mission in the Phase

To analyze the causes of system failures and mission failures, the FTA was used to model the system. FTA is a graphical deduction method for reliability, safety, usability analysis, and risk assessment of large and complex systems. The FT model is built by top events, intermediate events, basic events, and the logic gates that represent the logic of these three types of events. The top event is the system failure during each mission in the execution phase. Component failures that can cause system failures are regarded as the basic events of the FT model. Intermediate events are represented by subsystems containing these faulty components. After determining all events, different types of events are connected to the corresponding logic gates. Finally, the FT model of each mission is established. For example, the Phase I mission I-1 of the MM-PMS in Fig. 1 can be used to establish a fault tree model. Assuming components U1 and U2 form a subsystem, a failure of any of the three components will result in a system failure. Then, the FT model of Mission I-1 is shown in Fig. 4.

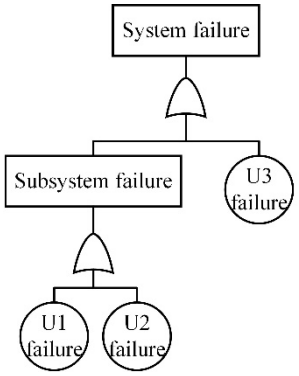


**Fig 4.** The FT model of mission I-1.

## 3.4. Module 4: Establishment of MM-PMS All-phase Continuous DBN-GO-FT Model

The MM-PMS all-phase continuous DBN-GO-FTA model is divided into the following four subsections.

### 3.4.1. Mapping the GO Model to BN for Each Phase

The equivalent model of GO operator mapping BN and its mapping algorithm is shown in Fig. 5. The equivalent BN models of the fifth type of operator and the first type of operator are represented by (a) and (b) in Fig. 5, respectively. In Fig. 5, P1 represents the probability of mission success, and P2 represents the probability of mission failure. 1 means that the current state has not changed, and 0 means that the current state has been changed. Only the previous mission successfully completes the next mission can continue, otherwise, it cannot continue. Operator 5-1 instructs the beginning of execution of the overall task of the system. 1-1 and 1-2 indicate mission I-1 and mission I-2 in Phase I separately.

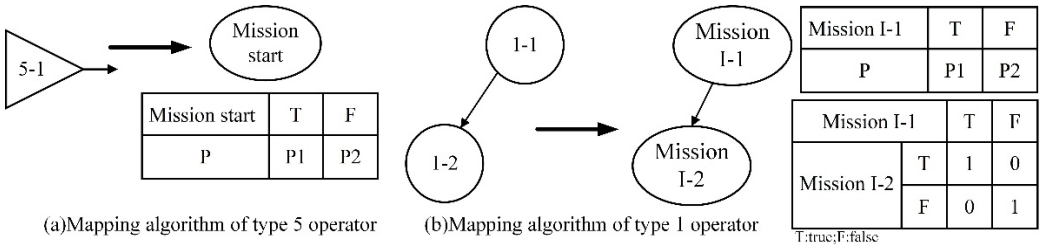


**Fig 5.** Mapping algorithm of GO operators to BN.

According to the above mapping method, the GO model in Fig. 3 is mapped to BN. Define the logical relationship between continuous missions according to the table in Fig. 5. (b), as shown in Fig. 6.

ISSN: 2688-8645

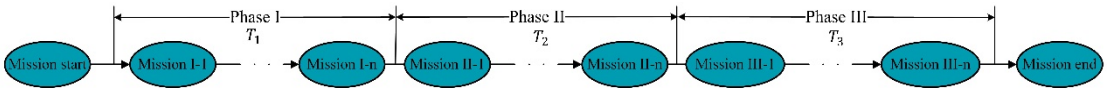


**Fig 6.** The BN model for MM-PMS concise example diagram.

### 3.4.2. Mapping the FT Model for Each Mission in the Phase into BN

This section uses the FT model of mission I-1 in Fig. 4 as an example to introduce the procedure of converting the FT model of each mission into an equivalent BN. The top event, intermediate event, and basic event in the FT model are respectively converted to child nodes, intermediate nodes, and parent nodes in BN (Liu et al., 2015). The meaning expressed by logic gates is defined by the conditional probability table (CPT) of intermediate nodes and child nodes. The FT conversion BN model of Mission I-1 is shown in Fig. 7. The conditional probability table in Fig. 7 is filled in according to the definition of the logical OR gate. The failure of any component will cause the system or subsystem to fail. The system is normal if and only if all components are normal.

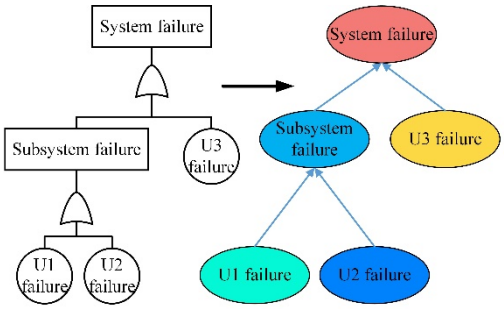


| U3 failure | | T | | F | |
|---|---|---|---|---|---|
| Subsystem failure | | T | F | T | F |
| System failure | T | 1 | 0 | 0 | 0 |
| | F | 0 | 1 | 1 | 1 |

| U1 failure | | T | | F | |
|---|---|---|---|---|---|
| U2 failure | | T | F | T | F |
| Subsystem failure | T | 1 | 0 | 0 | 0 |
| | F | 0 | 1 | 1 | 1 |

T:true;F:false

**Fig 7.** Mapping the FT model of mission I-1 to BN.

### 3.4.3. Establishment BN-GO-FT Model of Each Phase

Taking Phase I as an example, the BN mapped from the GO model is connected to the BN converted from the FT model of each mission in the phase. Finally, the BN-GO-FT model of Phase I is obtained. The human factors when performing missions are considered are represented by the corresponding nodes in BN. The updated BN-GO-FT model of Phase I is shown in Fig. 8. The emerald green nodes, light blue nodes, and yellow nodes represent the components of the system. Sky blue nodes represent subsystems. A gray node indicates that the node has been deactivated. The pink node indicates a system failure during the execution of the mission. Multiple missions in the phase are represented by dark green nodes. Human factors are represented by dark blue nodes.

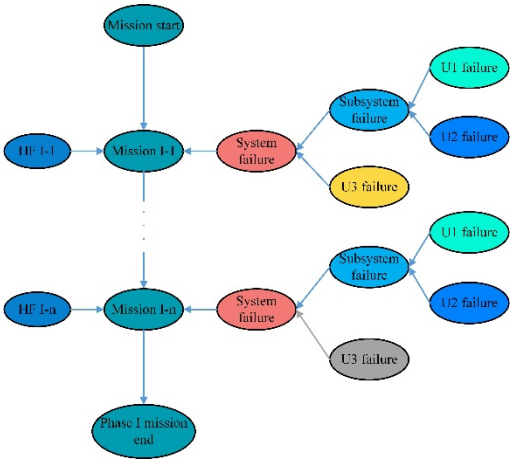


**Fig 8.** The BN-GO-FT model of Phase I.

ISSN: 2688-8645

### 3.4.4. Determine Node Parameters Phase Dependencies

When the operator performs each mission, HEP is quantified by SPAR-H, a human factor node, whose process is as follows:

1. Determine the type of mission.

2. Evaluate the impact of each PSF and determine the corresponding multiplier. The SPAR-H method has 8 PSFs, including available time, stressors, complexity, experience/training, procedures, ergonomics/human-machine interface (HMI), fitness for duty, and work process. The detailed information on each PSF parameter is introduced by Katrina M, Groth (Groth and Swiler, 2013).

3. Calculate the HEP of the mission. When the above work is completed, HEP is calculated by the following equations. Eq. 1 should be used when the actual error probability calculation value is less than 1. Otherwise, Eq. 2 should be applied.

$$HEP = NHEP \cdot \prod_1^8 PSF_i \quad (1)$$

$$HEP = NHEP \cdot \prod_1^8 PSF_i / [NHEP \cdot (\prod_1^8 PSF_I - 1) + 1] \quad (2)$$

where HEP is the probability of human error, nominal HEP (NHEP) is the nominal probability of error (NHEP=0.01 is diagnosis task, NHEP=0.001 is execution task), and $PSF_i$(i=1,2…8)is the multiplier for each PSF.

At the initial moment, the probability values of the node representing the component are 1, i.e., normal state, and 0, i.e., fault state. According to the conditions (2) set in Section 2, the current time is t and the time interval between two consecutive experiments is Δt. Then, the repair-free transition relationship between consecutive nodes can be determined. As shown in Table 1, λ represents the failure rate of the component (Nie et al., 2019). Equations in Table 1 are used to determine the transition probability tables representing system component nodes in DBN. The values of the conditional probability table of the child nodes and intermediate nodes in the DBN can be assigned according to the logical relationship. The phase dependencies of the system components have been defined in condition (4) of Section 2. Combining the working hours of each phase of MM-PMS, the BN-GO-FT model of each phase is extended to the DBN-GO-FT model. Then, the DBN-GO-FT model of each phase is connected. Then, the all-phase continuous DBN-GO-FT model of a concise example of MM-PMS is obtained in Fig. 9.

**Table 1.** Repair-free transition relationship between consecutive nodes.

| t | t+Δt | |
|---|---|---|
| | Normal | Fault |
| Normal | $e^{-\lambda\Delta t}$ | 0 |
| Fault | $1 - e^{-\lambda\Delta t}$ | 1 |

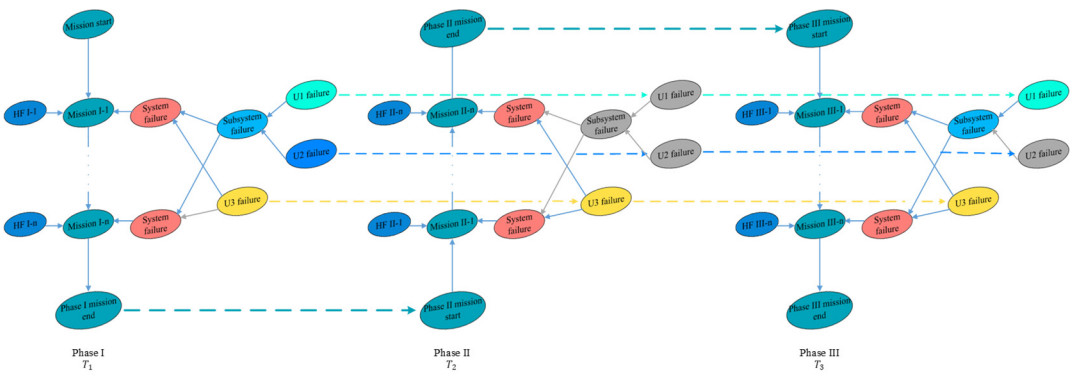


**Fig 9.** All-phase continuous DBN-GO-FT model of MM-PMS concise example.

ISSN: 2688-8645

### 3.5. Module 5: Reliability Assessment of the MM-PMS

In this module, based on the state probability values of all parent nodes in the model, the CPTs of intermediate and child nodes. Using the powerful information processing function of DBN, the success probability of the whole task of the system is calculated. The success probability of the whole task of the system reflects the probability that the MM-PMS will continue to run at the end of the whole task, that is, the reliability of MM-PMS.

## 4. Evaluate the Reliability of RLWI MM-PMS

### 4.1. Analysis of the RLWI System Performing P&A Tasks

This section describes in detail the structure of the RLWI system and the operational process for performing P&A tasks. The RLWI system consists of three main components as depicted in Fig. 10. As can be seen, a special dynamic positioning ship is equipped with an integrated control room and lifting device for operation. Wireline system for communication and control. The RLWI stack is composed of the pressure control head (PCH), lubricator section (LS), and well control package (WCP) connected in sequence. When the P&A task is started, the WCP is connected to the Horizontal X-mas tree (HXT).

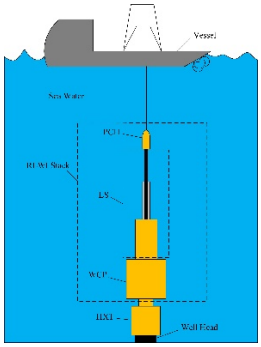


**Fig 10.** RLWI system.

The P&A task is divided into four phases, i.e., the preparatory phase, the reservoir abandonment phase, the intermediate abandonment phase, the wellhead and conductor removal phase. The duration of each phase is shown in Table 2. The operation process of each phase and the corresponding flow chart are shown in Fig. 11.

**Table 2.** The time required for the different phases.

| Different phases | Time required(h) |
|---|---|
| Phase 0:preparatory phase | 105 |
| Phase 1:reservoir abandonment | 60 |
| Phase 2: intermediate abandonment | 145 |
| Phase 3:wellhead and conductor removal | 35 |

Multiple missions can be included in one phase. Take the preparatory phase as an example, the missions are as follow:

Phase 0: preparatory phase:

1)P&A operation start

2)Install the RLWI stack and recycle the crown plug

3)Kill well

4)Install deep-set plug and perforate tubing

5)Circulate annulus and tubing clean

6)End of the preparatory phase

ISSN: 2688-8645

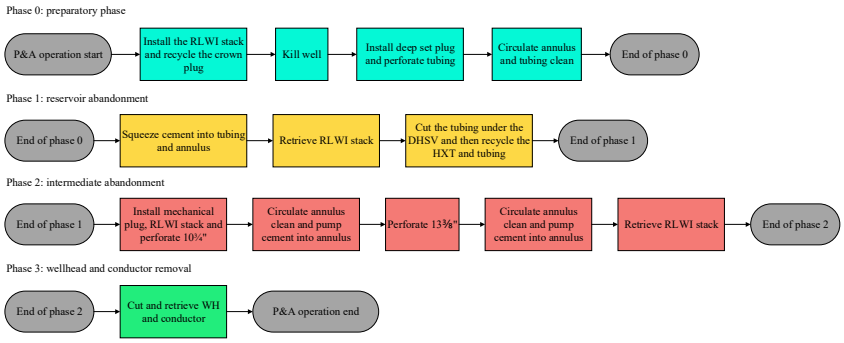


**Fig 11.** Flow chart of missions for each phase of P&A.

## 4.2. Establishment GO Models for Each Phase of the P&A Task

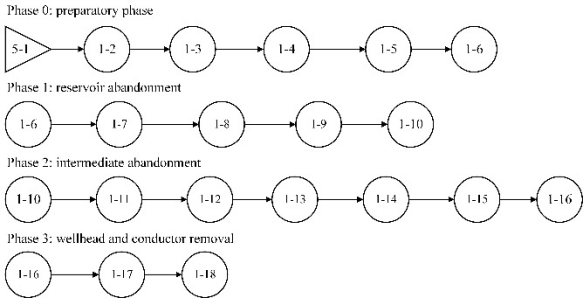


**Fig 12.** GO model for each phase of the P&A task

**Table 3.** The operation name and number of the BN nodes corresponding to the GO model.

| Operation name | The number of the GO model | BN nodes |
|---|---|---|
| P&A operation start | 5-1 | OS1 |
| Install the RLWI stack and recycle the crown plug | 1-2 | IO2 |
| Kill well | 1-3 | IO3 |
| Install deep-set plug and perforate tubing | 1-4 | IO4 |
| Circulate annulus and tubing clean | 1-5 | IO5 |
| End of Phase 0 | 1-6 | IO6 |
| Squeeze cement into tubing and annulus | 1-7 | IO7 |
| Retrieve RLWI stack | 1-8 | IO8 |
| Cut the tubing under the DHSV and then recycle the HXT and tubing | 1-9 | IO9 |
| End of Phase 1 | 1-10 | IO10 |
| Install mechanical plug, RLWI stack, and perforate 10 3/4″ | 1-11 | IO11 |
| Circulate annulus clean and pump cement into annulus | 1-12 | IO12 |
| Perforate 13 3/8″ | 1-13 | IO13 |
| Circulate annulus clean and pump cement into the annulus and main bore | 1-14 | IO14 |
| Retrieve RLWI stack | 1-15 | IO15 |
| End of Phase 2 | 1-16 | IO16 |
| Cut and retrieve WH and conductor | 1-17 | IO17 |
| P&A operation end | 1-18 | OE18 |

ISSN: 2688-8645

The P&A operation at the beginning can be regarded as an input signal. Only when the input signal appears, the task can continue to execute, represented by the operator of type 5. Each phase and the result of each mission in this phase have two states, i.e., success and failure, represented by the operator of type 1. The signal flow sequence is used to connect each operator once their operator type is determined. The GO model of each phase of the P&A task is shown in Fig. 12. Table 3 lists the specific meaning of each operator in the GO model at each phase.

## 4.3. Establishment FT Models for Each Mission of Each Phase

**Table 4.** List of the basic events in the fault tree during the P&A operation.

| Basic event | Description of basic events | Failure rate(λ) |
|---|---|---|
| X1 | Mechanical rubber element seals leakage | 0.34E-6/h |
| X2 | Structural deficiency of tool catcher on PCH | 0.35E-6/h |
| X3 | Cutting ball valve failure | 0.29E-6/h |
| X4 | Safe joint failure | 0.35E-6/h |
| X5 | Hydraulic pump failure | 0.11E-6/h |
| X6 | Shear ram Fail to function on demand | 0.12E-6/h |
| X7 | Accumulators failure | 0.14E-6/h |
| X8 | Controls module failure | 1.95E-6/h |
| X9 | Production isolation valve failure | 1.93E-6/h |
| X10 | Running tool failure | 5.28E-6/h |
| X11 | Lifting tools failure | 1.15E-5/h |
| X12 | Downhole safety valve failure | 1.06E-6/h |
| X13 | Gate valve failure | 0.44E-6/h |
| X14 | Kill line valve failure | 1.04E-6/h |
| X15 | Kill line leakage | 4.15E-5/h |
| X16 | Casing hangers leakage | 0.06E-6/h |
| X17 | Tubing hangers leakage | 0.22E-6/h |
| X18 | Wellhead connector leakage | 2.08E-5/h |
| X19 | Annulus master valve failure | 0.82E-6/h |
| X20 | Cross-over valve failure | 0.82E-6/h |
| X21 | Annulus vent valve failure | 0.82E-6/h |
| X22 | Annulus wing valve failure | 0.82E-6/h |
| X23 | Production main valve fail to open | 0.05E-6/h |
| X24 | Production main valve leakage | 0.17E-6/h |
| X25 | Production wing valve failure | 0.1E-6/h |
| X26 | Production choke valve plugged/choked | 0.43E-6/h |
| X27 | Cement pump failure | 3.01E-5/h |
| X28 | Cementing adaptor tool circulation inlet valve plugged/choked | 0.54E-6/h |
| X29 | Cementing adaptor tool circulation outlet valve plugged/choked | 0.54E-6/h |
| X30 | Cementing adaptor tool seals leakage | 0.11E-6/h |
| X31 | Cementing adaptor tool wiper plug leakage | 0.47E-6/h |
| X32 | Cement spool isolation plug leakage | 1.84E-6/h |
| X33 | Cement spool leakage | 0.13E-6/h |

The FT model of the RLWI system is obtained using the FTA method in Fig. 13. Each mission in the phase may only use part of the components or subsystems of the RLWI system in the execution process. The FT model of each mission (For details, please refer to Appendix A) can

ISSN: 2688-8645

be obtained by combining the influence of environmental factors in the mission execution process.

Based on OREDA (DNV, 2015) and data from papers published by Nan et al. (Pang et al., 2021) and Wang et al. (Wang et al., 2020), the failure rate of each basic event in the FT model of the RLWI system is listed in Table 4.

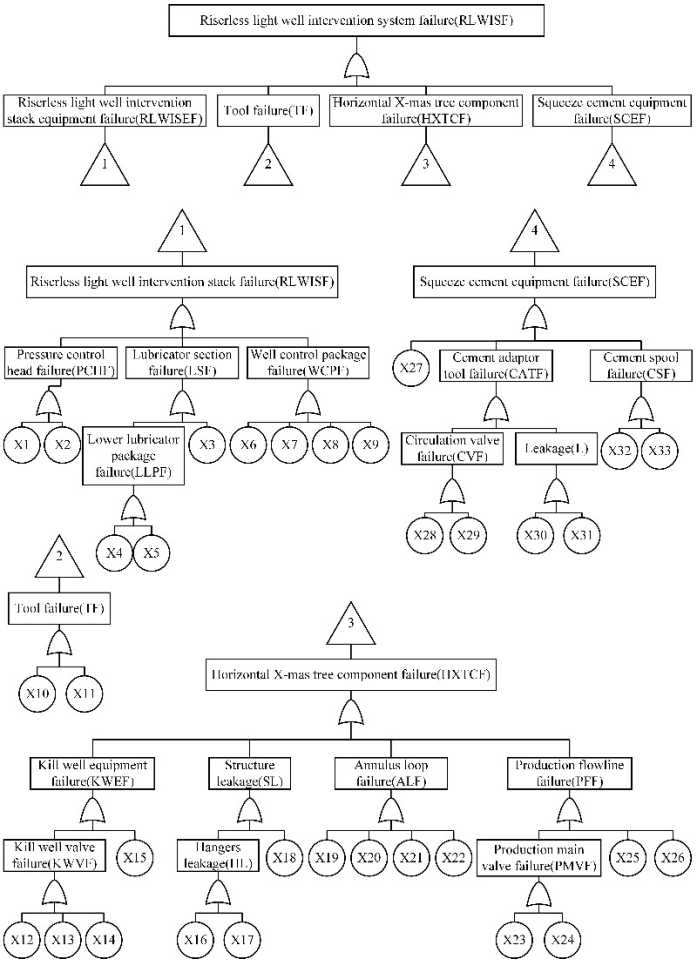


**Fig 13.** FT model of RLWI system.

## 4.4. Establishment of All-phase Continuous DBN-GO-FT Model of RLWI MM-PMS

According to the method presented in Section 3.4.4, the parameters of the human factor node and component node are determined in the model. This paper identifies all missions in P&A task execution as execution missions. Operators have received good training before performing various missions. Considering the complexity of each mission in the P&A process, the complexity level of the mission to retrieve the RLWI stack is considered to be nominal. The complexity level of the remaining missions is considered medium. The rest of the PSF levels for each mission are nominal. Table 5 shows the name of each mission operation and the corresponding BN node. Use Eq. 1 to calculate the HEP of each mission operation, as shown in Table 6. Based on the failure probability of each component in Table 4, the time interval is set to $\Delta t$=5h and the parameters of each component node are calculated using the equation in Table 1. In addition, according to the FT model of each mission, the logical value of the OR gate is used to allocate the CPT of the intermediate node and child nodes of the DBN. Based on the definition of phase dependence, phases in the P&A task are connected. Finally, according to the duration of each phase in Table 2, the all-phase continuous DBN-GO-FT model of RLWI MM-PMS is obtained, as shown in Fig 13.

ISSN: 2688-8645

**Table 5.** The name of each mission operation and the corresponding BN node.

| Mission operation name | BN node |
|---|---|
| The operation of install the RLWI stack and recycle the crown plug | HF1 |
| The operation of kill well | HF2 |
| The operation of install deep-set plug and perforate tubing | HF3 |
| The operation of circulating annulus and tubing clean | HF4 |
| The operation of squeeze cement into tubing and annulus | HF5 |
| The operation of retrieve RLWI stack | HF6 |
| The operation of cut the tubing under the DHSV and then recycle the HXT and tubing | HF7 |
| The operation of installing the mechanical plug, RLWI stack, and perforate 10 3/4“ | HF8 |
| The operation of circulate annulus clean and pump cement into the annulus | HF9 |
| The operation of perforate 13 3/8“ | HF10 |
| The operation of circulate annulus clean and pump cement into the annulus and main bore | HF11 |
| The operation of retrieve RLWI stack | HF12 |
| The operation of cut and retrieve WH and conductor | HF13 |

**Table 6.** Human error probability of each mission operation.

| | HF1 | HF2 | HF3 | HF4 | HF5 | HF6 | HF7 |
|---|---|---|---|---|---|---|---|
| Available time | 1 | 1 | 1 | 1 | 1 | 1 | 1 |
| Stressors | 1 | 1 | 1 | 1 | 1 | 1 | 1 |
| Complexity | 2 | 2 | 2 | 2 | 2 | 1 | 2 |
| Experience/training | 0.5 | 0.5 | 0.5 | 0.5 | 0.5 | 0.5 | 0.5 |
| Procedures | 1 | 1 | 1 | 1 | 1 | 1 | 1 |
| Ergonomics/HMI | 1 | 1 | 1 | 1 | 1 | 1 | 1 |
| Fitness for duty | 1 | 1 | 1 | 1 | 1 | 1 | 1 |
| Work processes | 1 | 1 | 1 | 1 | 1 | 1 | 1 |
| HEP | 0.001 | 0.001 | 0.001 | 0.001 | 0.001 | 0.0005 | 0.001 |
| | | | | | | | |
| | HF8 | HF9 | HF10 | HF11 | HF12 | HF13 | |
| Available time | 1 | 1 | 1 | 1 | 1 | 1 | |
| Stressors | 1 | 1 | 1 | 1 | 1 | 1 | |
| Complexity | 2 | 2 | 2 | 2 | 1 | 2 | |
| Experience/training | 0.5 | 0.5 | 0.5 | 0.5 | 0.5 | 0.5 | |
| Procedures | 1 | 1 | 1 | 1 | 1 | 1 | |
| Ergonomics/HMI | 1 | 1 | 1 | 1 | 1 | 1 | |
| Fitness for duty | 1 | 1 | 1 | 1 | 1 | 1 | |
| Work processes | 1 | 1 | 1 | 1 | 1 | 1 | |
| HEP | 0.001 | 0.001 | 0.001 | 0.001 | 0.0005 | 0.001 | |

## 4.5. Model Validation

In order to prove the correctness of the established DBN model, this paper uses another reliability analysis method Petri Net (PN) to verify the model (Volovoi, 2004). Because the model is large, the node TF and its parent nodes X10, X11 in phase 0 are selected for partial verification to illustrate the correctness of the model. The PN model of X10 and X11 are shown in Fig. 14. X10 normal and X11 fault respectively represent the two states of X10 node: “Normal” and “Fault”. T1 indicates that the node status changes from “Normal” to “Fault”. According to the established PN model and the Markov model containing two states (Yang et al., 2012), the state transition matrix $Q_i$ and steady-state probability distribution matrix $Y_i$ of nodes X10 and X11 are obtained.

ISSN: 2688-8645

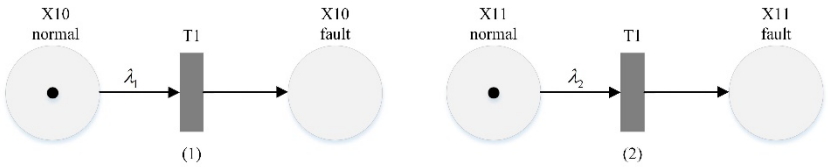


**Fig 14.** Petri net of X10 and X11.

$$Q_{X10} = \begin{bmatrix} -\lambda_1 & \lambda_1 \\ 0 & 0 \end{bmatrix} \tag{3}$$

$$Q_{X11} = \begin{bmatrix} -\lambda_2 & \lambda_2 \\ 0 & 0 \end{bmatrix} \tag{4}$$

$$Y_{X10} = \begin{bmatrix} e^{-\lambda_1 \Delta t} & 1 - e^{-\lambda_1 \Delta t} \\ 0 & 0 \end{bmatrix} \tag{5}$$

$$Y_{X11} = \begin{bmatrix} e^{-\lambda_2 \Delta t} & 1 - e^{-\lambda_2 \Delta t} \\ 0 & 0 \end{bmatrix} \tag{6}$$

The reliability value of each node can be obtained by formulas (5)~(6). The nodes X10 and X11 are connected to the node TF through a logical OR gate from a series system. So the reliability calculation formula of the series system can be used. The formula is as follows:

$$R_{TF} = R_{X10} \cdot R_{X11} = e^{-\lambda_1 \Delta t} \cdot e^{-\lambda_2 \Delta t} \tag{7}$$

The results are compared with the results of the DBN model, as shown in Fig. 15. The reliability values obtained by the two methods are basically the same, and the maximum relative error is only 2.9E-9%. The rationality of the DBN model is verified.

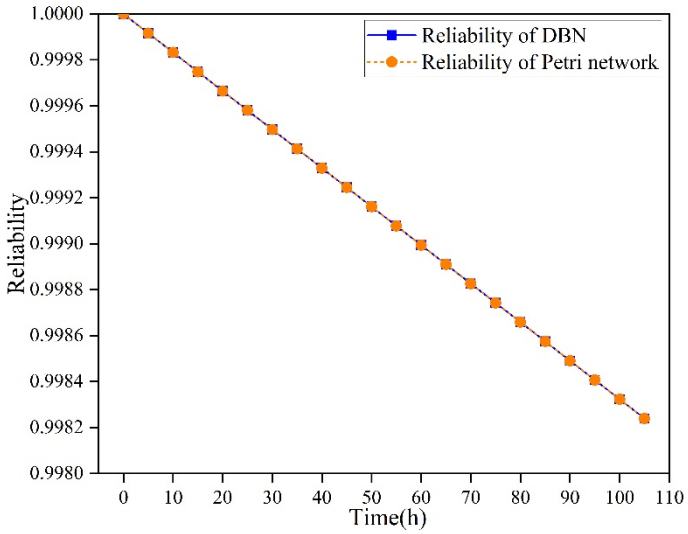


**Fig 15.** Verification results of DBN model.

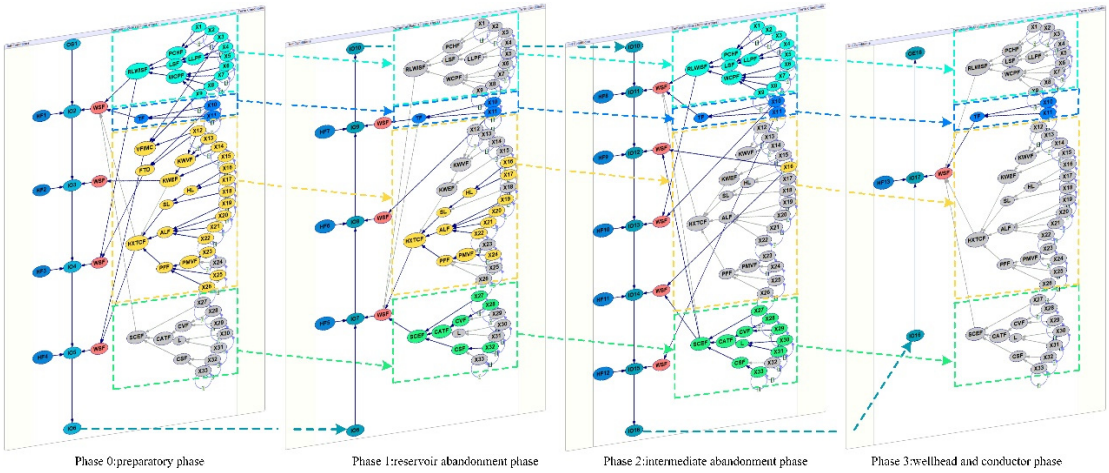


**Fig 16.** All-phase continuous DBN-GO-FT model of RLWI MM-PMS

ISSN: 2688-8645

# 5. Results and Discussions

## 5.1. Reliability Analysis

The established DBN-GO-FT model is used to analyze the reliability of RLWI MM-PMS. The relationship between system reliability and time is obtained in Fig. 17. The diagonal lines in the figure indicate the change in system reliability over time for each phase. The system reliability gradually decreases as the mission time increases. It is worth noting that there is a jump discontinuity between the reliability curves of each phase, which is due to the phase dependence of the system components, human error, and different configurations in different phases. In order to compare different conditions, the red line in Fig. 17 draws the system reliability considering only component factors, while the black one considers both component factors and human factors. The system reliability that considers only component factors is higher than that considers both component factors and human factors, which proves that human error hurts system reliability.

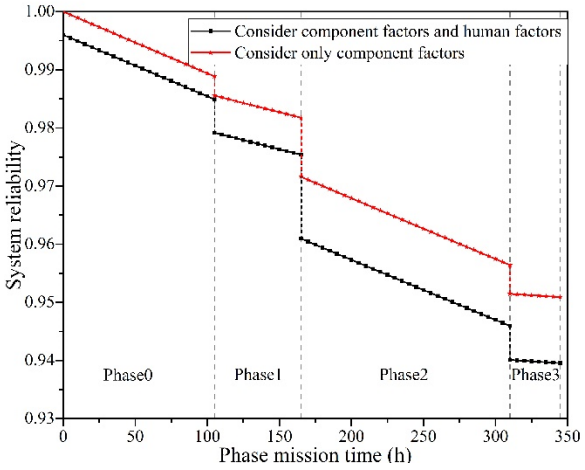


**Fig 17.** Reliability analysis results of RLWI MM-PMS.

## 5.2. The Influence of Human Factors and Component Factors

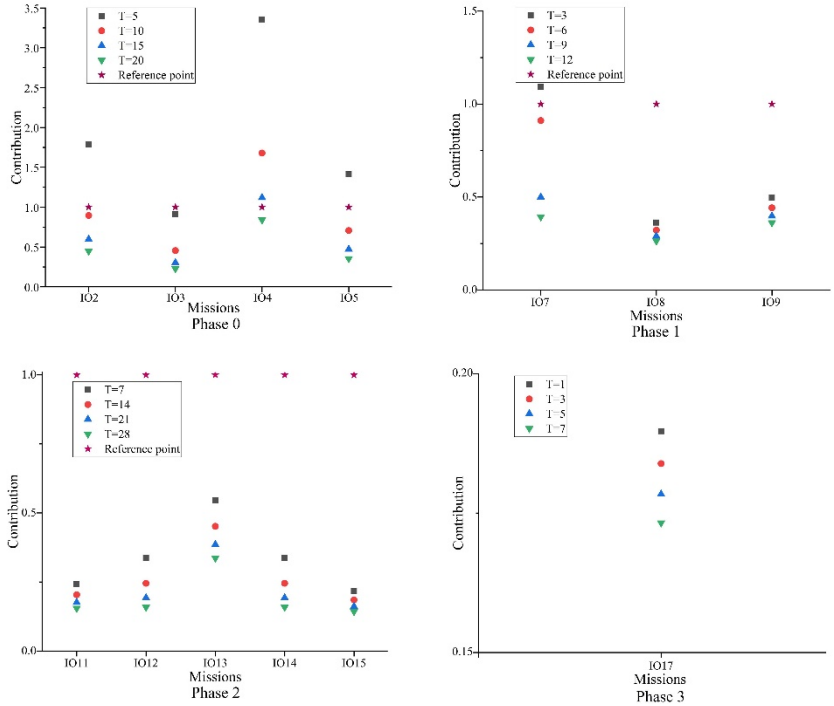


**Fig 18.** The degree of influence of human and component factors

ISSN: 2688-8645

When a mission fails at a specific time, the backward reasoning capabilities of BNs can be used to diagnose the influence of human error and component failure. Then, the posterior probabilities of each human factor node and component node are obtained. The ratio of the posterior probabilities of human factor nodes to component nodes is defined as the degree of influence on the occurrence of mission fails. When the ratio is greater than 1, the influence of human error will be greater. Conversely, component failure has a greater influence.

In Fig 18, each phase uses four-time slices for analysis and the reference point (contribution ratio = 1) represents human error and component failure have an identical effect on the system. As shown in the figure, the degree of influence of component failure increases with the increase of time. The human error only has a higher impact on the mission failure for IO2 (5 h), IO4 (5 h), IO4 (10 h), IO4 (15 h), IO5 (5h), IO 7 (3 h). It can be concluded that human error has a stronger effect than component failure at the early stage of IO2, IO4, IO5, IO7. On the other hand, component failures are usually more important in Phases 1, 2, and 3. It almost dominates the mission failure in Phase 3. As a result, managers can adjust personnel and components in real-time to prevent system failures.

## 6. Conclusion

This paper establishes the reliability model of RLWI MM-PMS based on DBN. The GO method is used to model the phase mission process, and the GO model of each phase is obtained. Establish the FT model of each mission in each phase to analyze the reasons that may lead to the failure of the mission. In addition, using SPAR-H to quantitatively analyze human factors and adding them to the DBN model improves the accuracy of the model. Finally, the reliability of the RLWI MM-PMS for oil well P&A operations is analyzed. The conclusion can be summarized as: In the DBN-GO-FT reliability analysis of RLWI MM-PMS, the human factor reduces the system reliability with time. In Phase 1, 2, and 3, the component factors have a higher impact on the system reliability, especially in Phase 3. On the other hand, human factors can have a higher influence at the beginning of Phase 0. Overall, the influence of human factors decreases with time.

## References

[1] Alam, M., Al-Saggaf, U.M., 1986. Quantitative Reliability Evaluation of Repairable Phased-Mission Systems Using Markov Approach. IEEE Trans. Reliab. 35, 498–503. https:// doi.org/ 10.1109 /TR. 1986. 4335529.

[2] Babaleye, A.O., Kurt, R.E., Khan, F., 2019. Safety analysis of plugging and abandonment of oil and gas wells in uncertain conditions with limited data. Reliab. Eng. Syst. Saf. 188, 133–141. https:// doi.org/ https://doi.org/10.1016/j.ress.2019.03.027.

[3] Bobbio, A., Portinale, L., Minichino, M., Ciancamerla, E., 2001. Improving the analysis of dependable systems by mapping fault trees into Bayesian networks. Reliab. Eng. Syst. Saf. 71, 249–260. https:// doi. org/ https://doi.org/10.1016/S0951-8320(00)00077-6.

[4] Chen, D., Fan, Y., Li, W., Wang, Y., Zhang, S., 2019. Human reliability prediction in deep-sea sampling process of the manned submersible. Saf. Sci. 112, 1–8. https:// doi.org/ https:// doi.org /10. 1016/ j. ssci. 2018.10.001.

[5] Cooper, S.E., Ramey-Smith, A.M., Wreathall, J., Parry, G.W., 1996. A technique for human error analysis (ATHEANA). Nuclear Regulatory Commission.

[6] Desmorat, G., Guarnieri, F., Besnard, D., Desideri, P., Loth, F., 2013. Pouring CREAM into natural gas: The introduction of Common Performance Conditions into the safety management of gas networks. Saf. Sci. 54, 1–7. https://doi.org/https://doi.org/10.1016/j.ssci.2012.10.008.

[7] DNV, G.L., 2015. Offshore reliability data handbook (OREDA). Det Nor. Verit. DNV, Hovik, Norw.

ISSN: 2688-8645

[8] Forester, J.A., Ramey-Smith, A., Bley, D.C., Kolaczkowski, A.M., Cooper, S.E., Wreathall, J., 1998. Discussion of comments from a peer review of a technique for human event analysis (ATHEANA). Sandia National Laboratories.

[9] Groth, K.M., Swiler, L.P., 2013. Bridging the gap between HRA research and HRA practice: A Bayesian network version of SPAR-H. Reliab. Eng. Syst. Saf. 115, 33–42. https://doi.org/ https:// doi.org/ 10. 1016/ j.ress.2013.02.015.

[10] Hameed, A., Khan, F., Ahmed, S., 2016. A risk-based shutdown inspection and maintenance interval estimation considering human error. Process Saf. Environ. Prot. 100, 9–21. https:// doi.org/ https: // doi.org/10.1016/j.psep.2015.11.011.

[11] Jahangiri, M., Hoboubi, N., Rostamabadi, A., Keshavarzi, S., Hosseini, A.A., 2016. Human Error Analysis in a Permit to Work System: A Case Study in a Chemical Plant. Saf. Health Work 7, 6–11. https:// doi.org/https://doi.org/10.1016/j.shaw.2015.06.002.

[12] Khakzad, N., Khan, F., Amyotte, P., 2013. Dynamic safety analysis of process systems by mapping bow-tie into Bayesian network. Process Saf. Environ. Prot. 91, 46–53. https:// doi.org/ https:// doi. org/ 10.1016/j.psep.2012.01.005.

[13] La Band, R.A., Andrews, J.D., 2004. Phased mission modelling using fault tree analysis. Proc. Inst. Mech. Eng. Part E J. Process Mech. Eng. 218, 83–91. https:// doi.org /10. 1243/ 09544080477413 4262.

[14] Li, X., Zhang, Y., Abbassi, R., Khan, F., Chen, G., 2021. Probabilistic fatigue failure assessment of free spanning subsea pipeline using dynamic Bayesian network. Ocean Eng. 234, 109323. https:// doi. org/ https://doi.org/10.1016/j.oceaneng.2021.109323.

[15] Liu, D., Zhang, C., Xing, W., Li, R., 2008. Reliability analysis of phased-mission systems using Bayesian networks, in: 2008 Annual Reliability and Maintainability Symposium. IEEE, pp. 21–26.

[16] Liu, P., Liu, Y., Cai, B., Wu, X., Wang, K., Wei, X., Xin, C., 2020. A dynamic Bayesian network based methodology for fault diagnosis of subsea Christmas tree. Appl. Ocean Res. 94, 101990. https: //doi. org/ https://doi.org/10.1016/j.apor.2019.101990.

[17] Liu, Z., Liu, Y., Cai, B., Zhang, D., Zheng, C., 2015. Dynamic Bayesian network modeling of reliability of subsea blowout preventer stack in presence of common cause failures. J. Loss Prev. Process Ind. 38, 58–66. https://doi.org/https://doi.org/10.1016/j.jlp.2015.09.001.

[18] Liu, Z., Liu, Y., Wu, X. lei, Cai, B., 2018. Risk analysis of subsea blowout preventer by mapping GO models into Bayesian networks. J. Loss Prev. Process Ind. 52, 54–65. https:// doi. org/ https: // doi. org/ 10.1016/j.jlp.2018.01.014.

[19] Liu, Z., Ma, Q., Cai, B., Liu, Y., Zheng, C., 2021. Risk assessment on deepwater drilling well control based on dynamic Bayesian network. Process Saf. Environ. Prot. 149, 643–654. https:// doi.org/ https: //doi.org/10.1016/j.psep.2021.03.024.

[20] Matsuoka, T., Kobayashi, M., 1988. GO-FLOW: a new reliability analysis methodology. Nucl. Sci. Eng. 98, 64–78.

[21] Moeinikia, F., Fjelde, K.K., Saasen, A., Vrålstad, T., Arild, Ø., 2015. A probabilistic methodology to evaluate the cost efficiency of rigless technology for subsea multiwell abandonment. SPE Prod. Oper. 30, 270–282.

[22] Mura, I., Bondavalli, A., 2001. Markov regenerative stochastic petri nets to model and evaluate phased mission systems dependability. IEEE Trans. Comput. 50, 1337–1351. https:// doi.org /10. 1109 /TC.2001.970572.

[23] Nie, Z., Chang, Y., Liu, X., Chen, G., 2019. A DBN-GO approach for success probability prediction of drilling riser emergency disconnect in deepwater. Ocean Eng. 180, 49–59. https:// doi.org/ https:// doi. org/ 10.1016/j.oceaneng.2019.04.005.

[24] Øia, T.M., Aarlott, M.M., Vrålstad, T., 2018. Innovative approaches for full subsea P&A create new opportunities and cost benefits, in: SPE Norway One Day Seminar. OnePetro.

[25] Pang, N., Jia, P., Wang, L., Yun, F., Wang, G., Wang, X., Shi, L., 2021. Dynamic Bayesian network-based reliability and safety assessment of the subsea Christmas tree. Process Saf. Environ. Prot. 145, 435–446. https://doi.org/https://doi.org/10.1016/j.psep.2020.11.026.

[26] Peng, R., Wu, D., Xiao, H., Xing, L., Gao, K., 2019. Redundancy versus protection for a non-reparable phased-mission system subject to external impacts. Reliab. Eng. Syst. Saf. 191, 106556. https:// doi.org/ https://doi.org/10.1016/j.ress.2019.106556.

[27] Purba, J.H., Tjahyani, D.T.S., 2016. Human reliability analysis in nuclear power plants, in: Proceeding Seminar National Technology Energy Nuclear. pp. 409–415.

[28] Standard, N., 2004. Well integrity in drilling and well operations. D-010, rev 3.

[29] Tang, Z., Dugan, J.B., 2006. BDD-based reliability analysis of phased-mission systems with multimode failures. IEEE Trans. Reliab. 55, 350–360. https://doi.org/10.1109/TR.2006.874941.

[30] Vaez, N., Nourai, F., 2013. RANDAP: An integrated framework for reliability analysis of detailed action plans of combined automatic-operator emergency response taking into account control room operator errors. J. Loss Prev. Process Ind. 26, 1366–1379. https://doi.org/ https:// doi.org/ 10. 1016/j.jlp.2013.08.011.

[31] Volovoi, V., 2004. Modeling of system reliability Petri nets with aging tokens. Reliab. Eng. Syst. Saf. 84, 149–161. https://doi.org/https://doi.org/10.1016/j.ress.2003.10.013.

[32] Wang, A., Luo, Y., Tu, G., Liu, P., 2011. Quantitative Evaluation of Human-Reliability Based on Fuzzy-Clonal Selection. IEEE Trans. Reliab. 60, 517–527. https://doi.org/10.1109/TR.2011.2161031.

[33] Wang, C., Liu, Y., Hou, W., Wang, G., Zheng, Y., 2020. Reliability and availability modeling of Subsea Xmas tree system using Dynamic Bayesian network with different maintenance methods. J. Loss Prev. Process Ind. 64, 104066. https://doi.org/https://doi.org/10.1016/j.jlp.2020.104066.

[34] Wang, C., Liu, Y., Yu, C., Zheng, Y., Wang, G., 2021. Dynamic risk analysis of offshore natural gas hydrates depressurization production test based on fuzzy CREAM and DBN-GO combined method. J. Nat. Gas Sci. Eng. 91, 103961. https://doi.org/https://doi.org/10.1016/j.jngse.2021.103961.

[35] Wang, Y., Wang, K., Wang, T., Li, X.Y., Khan, F., Yang, Z., Wang, J., 2021. Reliabilities analysis of evacuation on offshore platforms: A dynamic Bayesian Network model. Process Saf. Environ. Prot. 150, 179–193. https://doi.org/https://doi.org/10.1016/j.psep.2021.04.009.

[36] Xu, Z., Mo, Y., Liu, Y., Jiang, T., 2019. Reliability assessment of multi-state phased-mission systems by fusing observation data from multiple phases of operation. Mech. Syst. Signal Process. 118, 603–622. https://doi.org/https://doi.org/10.1016/j.ymssp.2018.08.064.

[37] Yang, N., Yu, H., Qian, Z., Sun, H., 2012. Modeling and quantitatively predicting software security based on stochastic Petri nets. Math. Comput. Model. 55, 102–112.

[38] Zupei, S., Jia, G., Xiangrui, H., 2001. An exact algorithm dealing with shared signals in the GO methodology. Reliab. Eng. Syst. Saf. 73, 177–181. https://doi.org/https://doi.org/10.1016/S0951-8320 (01)00035-7.

## Appendix A

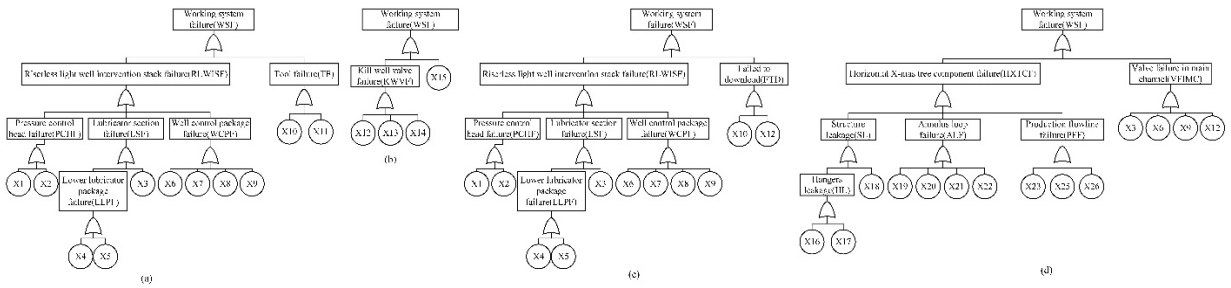

**Fig. A.1.** Working system FT model of each mission in phase 0: (a) Mission IO2; (b) Mission IO3; (c) Mission IO4; (d) Mission IO5.

**ISSN: 2688-8645**

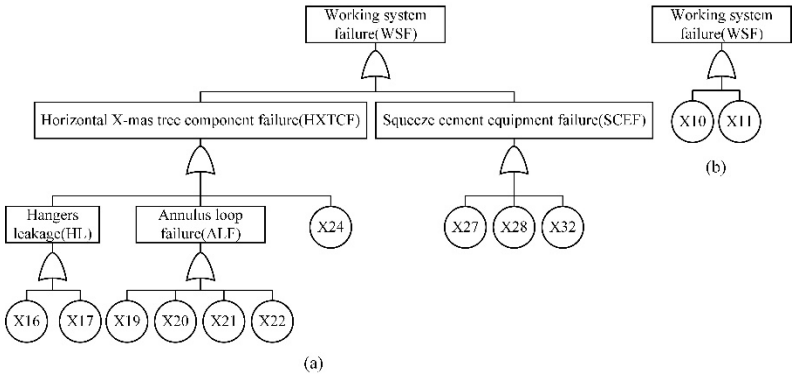


**Fig. A.2.** Working system FT model of each mission in phase 1: (a) Mission IO7; (b) Mission IO9.

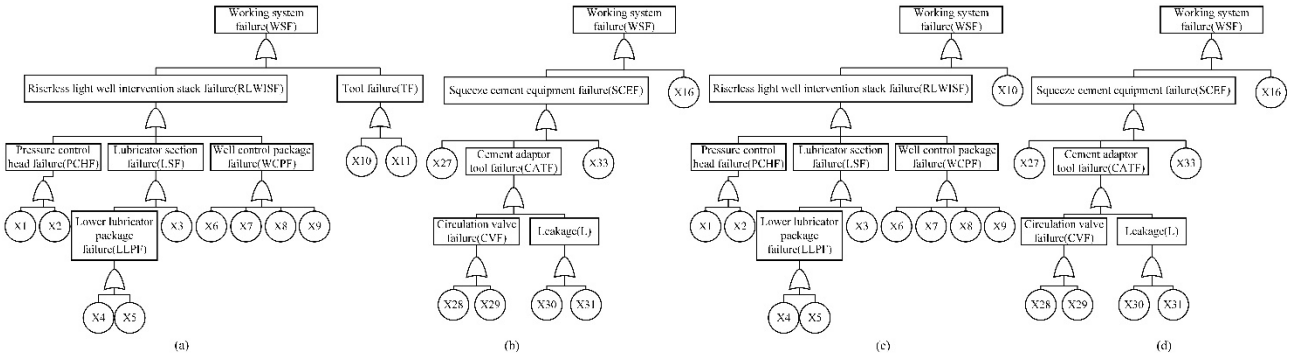


**Fig. A.3.** Working system FT model of each mission in phase 2: (a) Mission IO11; (b) Mission IO12; (c) Mission IO13; (d) Mission IO14.

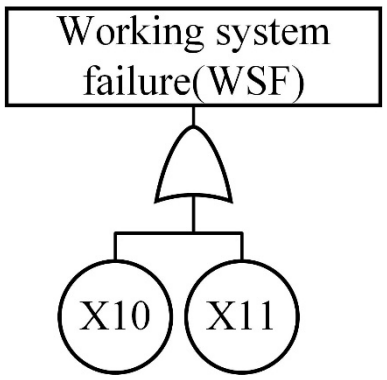


**Fig. A.4.** Working system FT model of mission IO17 in phase 3.